

Geochemistry of Darwin glass and target rocks from Darwin crater, Tasmania, Australia

Kieren T. HOWARD

School of Earth Sciences, University of Tasmania, Hobart, Tasmania 7000, Australia

Present address: Impacts and Astromaterials Research Centre, Department of Mineralogy, The Natural History Museum, Cromwell Road, London SW7 5BD, UK

Corresponding author. E-mail: kieren.howard@nhm.ac.uk

(Received 1 March 2007; revision accepted 25 July 2007)

Abstract—Darwin glass formed about 800,000 years ago in western Tasmania, Australia. Target rocks at Darwin crater are quartzites and slates (Siluro-Devonian, Eldon Group). Analyses show 2 groups of glass. Average group 1 is composed of: SiO₂ (85%), Al₂O₃ (7.3%), TiO₂ (0.05%), FeO (2.2%), MgO (0.9%), and K₂O (1.8%). Group 2 has lower average SiO₂ (81.1%) and higher average Al₂O₃ (8.2%). Group 2 is enriched in FeO (+1.5%), MgO (+1.3%) and Ni, Co, and Cr. Average Ni (416 ppm), Co (31 ppm), and Cr (162 ppm) in group 2 are beyond the range of sedimentary rocks. Glass and target rocks have concordant REE patterns (La/Lu = 5.9–10; Eu/Eu* = 0.55–0.65) and overlapping trace element abundances. ⁸⁷Sr/⁸⁶Sr ratios for the glasses (0.80778–0.81605) fall in the range (0.76481–1.1212) defined by the rock samples. ε-Nd results range from –13.57 to –15.86. Nd model ages range from 1.2–1.9 Ga (CHUR) and the glasses (1.2–1.5 Ga) fall within the range defined by the target samples. The ⁸⁷Sr/⁸⁶Sr versus ⁸⁷Rb/⁸⁶Sr regression age (411 ± 42 Ma) and initial ratio (0.725 ± 0.016), and the initial ⁴³Nd/¹⁴⁴Nd ratio (0.51153 ± 0.00011) and regression age (451 ± 140 Ma) indicate that the glasses have an inherited isotopic signal from the target rocks at Darwin crater. Mixing models using target rock compositions successfully model the glass for all elements except FeO, MgO, Ni, Co, and Cr in group 2. Mixing models using terrestrial ultramafic rocks fail to match the glass compositions and these enrichments may be related to the projectile.

INTRODUCTION

Darwin glass is a siliceous impact glass found in a strewn field covering more than 400 km² in western Tasmania, Australia. The glass also appears across the state in middens and caves formerly visited by Tasmanian Aboriginals who are the traditional owners of the glass. Darwin glass has been repeatedly dated at ~800 ka (Gentner et al. 1973) and our most recent age estimate of 816 ± 7 ka was determined by Ar-Ar methods (Loh et al. 2002). Ford (1972; his Fig. 1) identified a small (diameter = 1.2 km) circular depression near to the eastern edge of the strewn field in the Southwest World Heritage Area (42°18.39'S, 145°39.41'E). This pronounced topographic feature was named Darwin crater and assumed to be the source of Darwin glass, despite a lack of conclusive evidence and a paucity of data on the glass or crater. The origin of Darwin glass has been investigated in a Ph.D. thesis (Howard 2004) and this paper stems from that work. The geology of Darwin crater has been described in a detailed petrographic study and is consistent with that

expected in small simple impact craters formed in sedimentary target rocks (Howard and Haines 2007). Glass distribution data are consistent with ejection from Darwin crater and show: 1) the largest recovered fragments are found closest to the crater, 2) a decrease in the abundance glass fragments away from the crater, and 3) an increase in the proportion of splashform, relative to irregular or ropy, shapes away from the crater (Howard and Haines 2003; Howard 2004).

Impact glasses and tektites inherit the isotopic and geochemical signals of the source rocks melted during their formation. The aim of this paper is to test the compatibility of the suspected target rocks at Darwin crater as the materials melted under impact conditions to form Darwin glass. Most impact glasses and tektites have a composition similar to average upper continental crust and, as such, major- and trace-element composition alone is rarely enough to conclusively relate a glass to a suspected target rock or to define an impact origin. However, such investigations can effectively rule a suspected target rock in or out of further consideration in

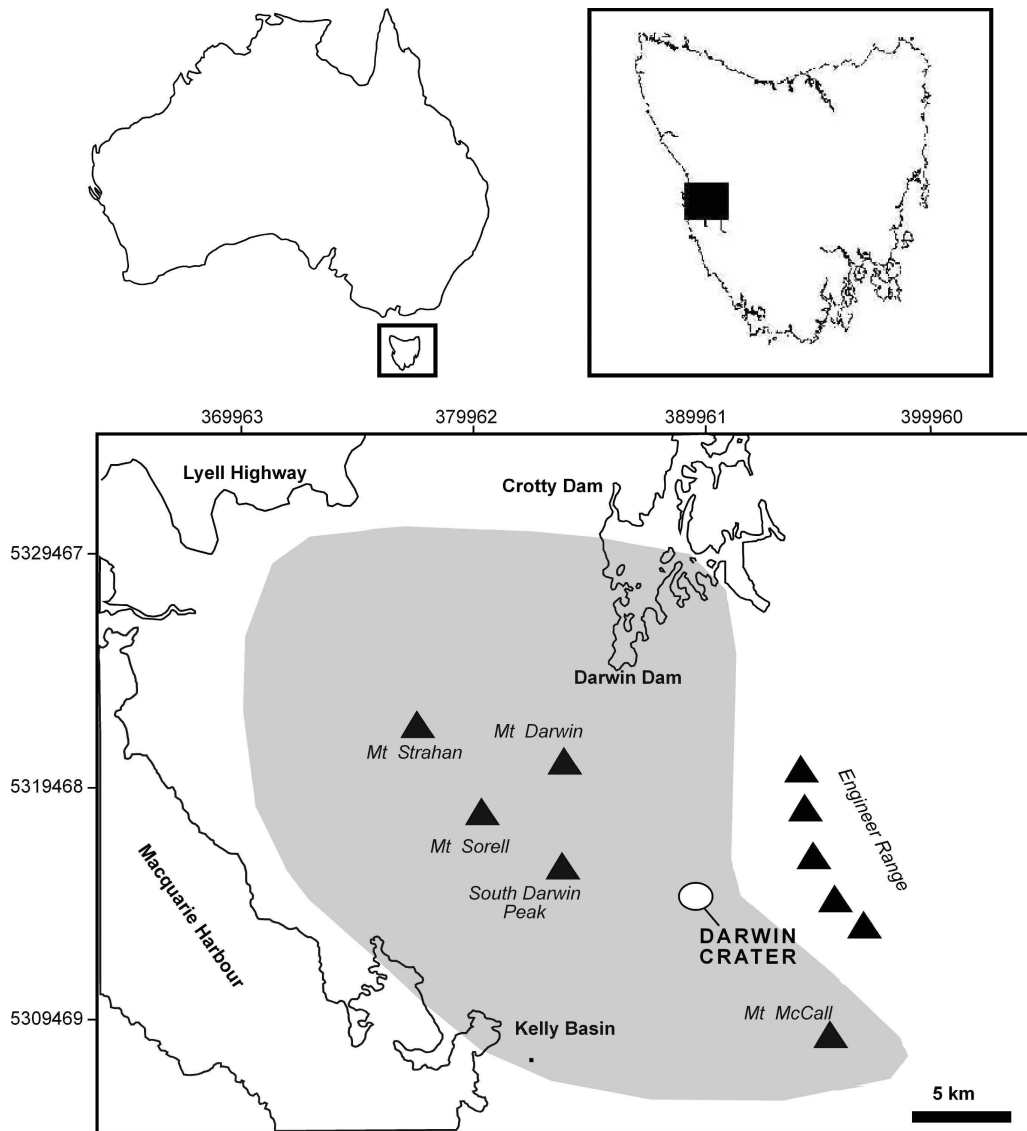


Fig. 1. Darwin crater and Darwin glass strewn field. The grey shaded area defines the Darwin glass strewn field.

studies aimed at defining the impact origin of a glass. In this paper, the geochemical and Sr,Nd isotopic systematics in Darwin glass are shown to be compatible with the suspected target rocks at Darwin crater.

STRATIGRAPHY

Darwin crater is situated on the Queenstown 1:250,000 scale geological map sheet (Corbett and Brown 1975; Fig. 2), which shows significant geological complexity across the area of the strewn field. The densely rainforested valley where Darwin crater lies is a tributary of the Andrew River valley. The Andrew River valley cuts into Ordovician limestone (Gordon Group). Siliceous conglomerate (Denison Group), unconformably dipping off Proterozoic quartzite of the Engineer Range, forms the east side of the valley, and Silurian

quartzite the west. Rocks at the crater are correlates of the Eldon Group; a succession of low-grade metasedimentary rocks consisting of quartzites and slates (Fig. 3). Gould (1866) first named these rocks the "Eldon Beds" and defined them as the rocks overlying the main limestone succession (Gordon Group), near the mouth of the Gordon and along the Eldon Rivers. Gill and Banks (1950) formally defined the Eldon Group and the following formations are recognized: (top) Bell Shale; Florence Sandstone; Keel Quartzite; Amber Slate and Crotty Quartzite (base, Fig. 3). The metamorphic grade of the rocks is lower greenschist, with the development of aligned micas that define the foliation cleavage of the slate units. In some samples, minor (<2%) chlorite alteration is also observed.

Two drill holes penetrate the center of the crater. The deepest hole penetrated to a depth of ~230 m. Drill cores intersected fine-grained lacustrine sediments (~60 m thick),

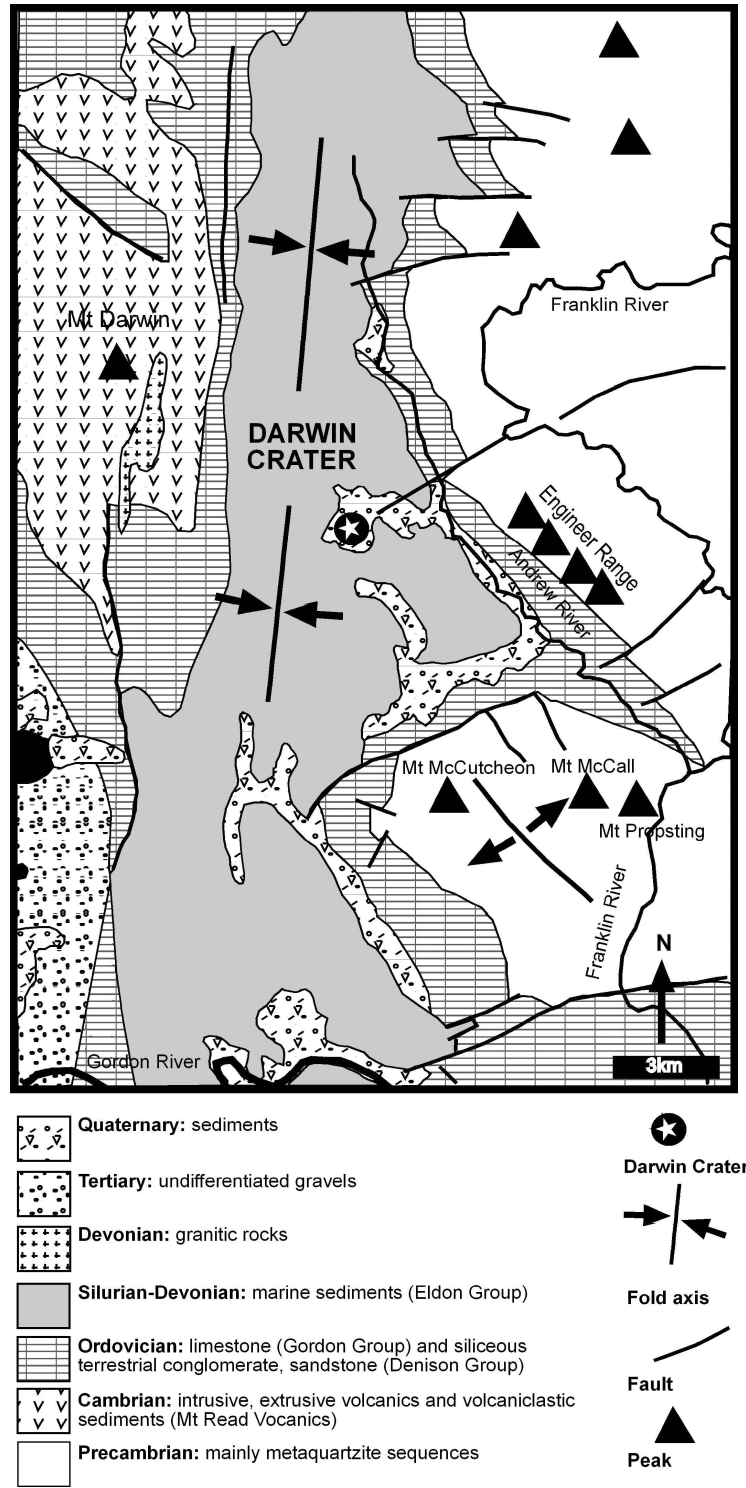


Fig. 2. Geology of the Darwin glass strewn field. Based on Corbett and Brown (1975) and Corbett et al. (1993).

overlying poorly sorted coarser crater-fill deposits. The pre-lacustrine crater-fill comprises a complicated package of angular polymict breccias of quartz and country rock with very rare glass, monomict sandy breccias of angular quartz, and clasts of deformed slate. The degree of deformation evident in

crater-fill samples is far greater than in rocks surrounding the crater but diagnostic shock indicators (e.g., planar deformation features [PDFs] in quartz grains) have not been observed. The petrographic features of the suspected target rocks and crater-fill samples are described in detail in Howard and Haines (2007).

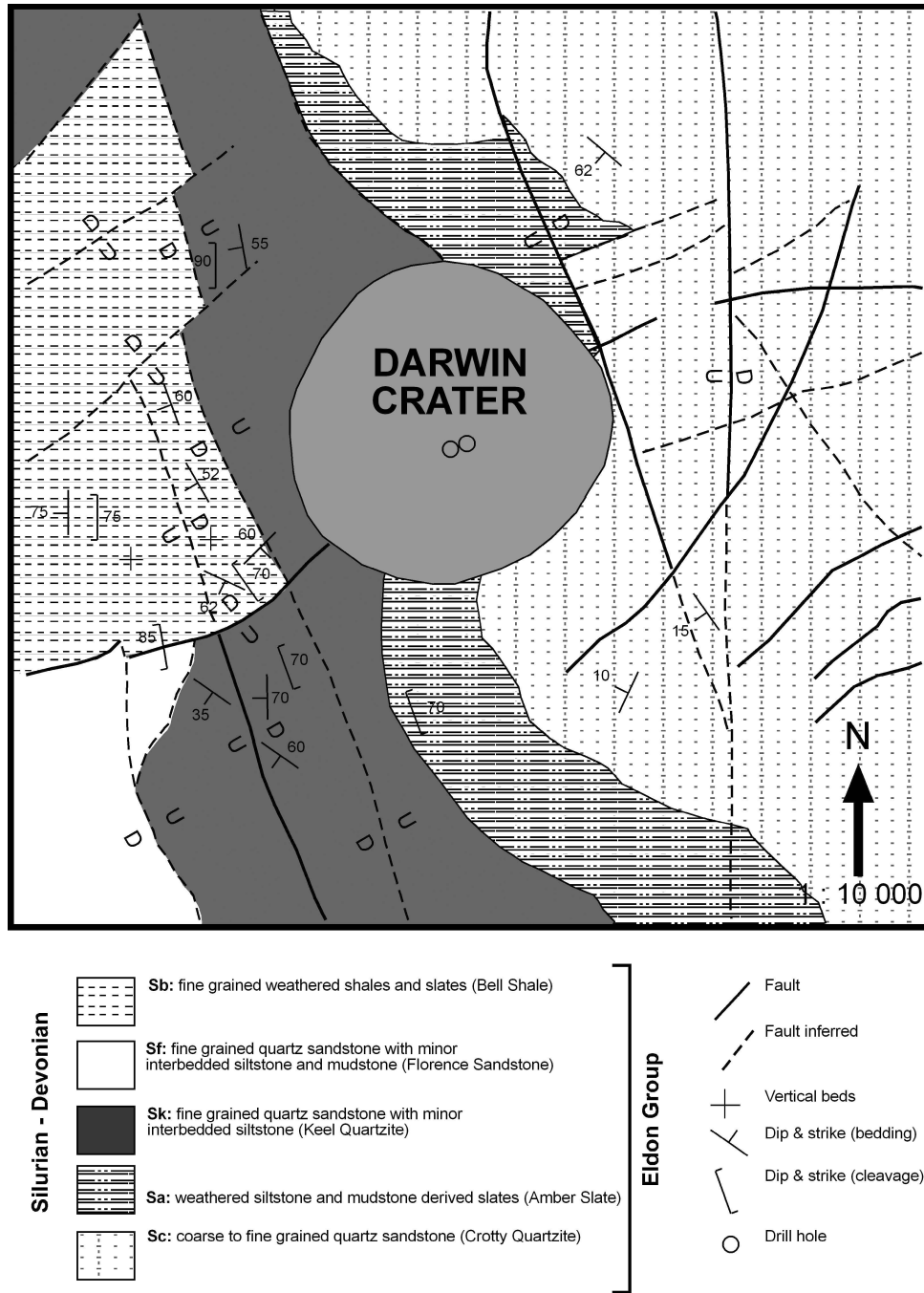


Fig. 3. Darwin crater geology. Based on field mapping in this study and by R. J. Ford; 1:25,000 scale aerial photographs; Corbett and Brown (1975) and Corbett et al. (1993).

METHODOLOGY

Scanning Electron Microscopy (SEM)

Small pieces of Darwin glass were carefully chipped from individual larger fragments and placed in an ultrasonic bath in distilled water for cleaning. The studied glass fragments were collected from across the strewn field. The detached pieces' sizes ranged from 2 to 10 mm in diameter

and these were mounted in epoxy discs 25 mm in diameter. In addition, 26 glass samples <5 mm in size and showing splashform (droplet, spheroid, and elongate) shapes (Fig. 4) were collected from across the strewn field, cleaned, and mounted intact in 25 mm epoxy discs. These “mini-glass” grains were polished carefully to expose a fresh interior surface for analysis. This is the first time such splashform mini-glass samples of Darwin glass have been reported or analyzed.



Fig. 4. Splashform Darwin mini-glasses. Scale bar = 1 cm.

Major elements were determined using a CAMECA SX50 scanning electron microscope, in WDS mode, at the Central Science Laboratory (CSL), University of Tasmania. The regulated electron beam current was operated at 25 nA at an accelerating voltage of 15 kV. A nominal incident beam size of 8 μm diameter was used in order to minimize alkali migration and consequent elevation of Si and Al counts. Eight major elements (Si, Al, Fe, Mg, Ti, K, Ca, Na) were analyzed using the mineral standards and calibrations provided by Dr. D. A. Steele. Detection limits range between 0.05 and 0.1 wt%. Sodium was analyzed first to reduce the effect of volatilization on the analysis. 2 spots were analyzed on each of the glass chips ($n = 216$). For the <5 mm mini-glasses, three spots were analyzed on each grain ($n = 78$). This results in a total of 294 analyses and significantly expands the published analyses of Darwin glass, the next largest study being Meisel et al. (1990), who analyzed 18 samples. Howard (2004) also contains more than 1000 other glass analyses from grid surveys on individual glass fragments.

Laser Ablation Inductively Coupled Plasma Mass Spectrometry (LA-ICPMS)

The same 25 mm epoxy discs containing Darwin glass fragments that were analyzed by SEM were analyzed for trace element compositions using LA-ICPMS. The School of Earth Sciences at the University of Tasmania uses an Merchantek 266 nm laser operated at 10 HZ and 3–6 J/cm² per pulse and the Agilent HP 4500 ICP-MS. 23 elements were determined during each analysis and these were: Cs, Rb, U, Th, Ba, La, Ce, Nb, Pr, Sr, Nd, Zr, Sm, Eu, Gd, Ho, Yb, Y, Lu, Sc, Cr, Co, and Ni. A nominal beam size of 120 μm was used throughout all analyses. Again two spots were analyzed on each glass chip for a total of 216 analyses. Each of the 26 mini-glasses were analyzed at four points each. Relative element sensitivities were calibrated against the glass standard NIST

612, and the standard BCR-2 was analyzed as an unknown. During the analyses, two analyses of both NIST 612 and BCR-2 were made before ten analyses of Darwin glass, followed by two more analyses each of NIST 612 and BCR-2. As an internal standard the measured intensity of ⁴⁹Ti during each analysis was normalized to the TiO₂ content of each glass determined previously by SEM. Throughout the course of the study, detection limits were between 0.1 and 0.001 ppm. Spectra for data presented here are flat and smooth with little deviation in counts per second throughout the 60 s duration of each analysis. This is generally the case in analyses of tektites and impact glasses that are well suited to the LA-ICPMS technique, especially for determination of refractory elements (rare earth elements [REE], Sr).

Suspected Target Rock Sample Selection and Preparation

In total, 33 samples that encompass the range of Eldon Group rocks found around the crater and throughout the drill cores were selected for analysis. Most of the analyzed surface samples were collected along a W-E traverse from the access track, to the eastern edge of the valley hosting the buried crater. These samples were collected in situ within the dense forest and not from bulldozer scrapings at the tracks edge or sampled regionally. The Crotty Quartzite formation is mappable from air photos but sampling the lithology very near to the crater is next to impossible owing to a lack of outcrop and the extreme vegetation at the eastern edge of the crater. For detailed chemical analyses (e.g., Sm, Nd isotopes), only stratigraphically constrained samples of Keel Quartzite and Amber Slate from the craters edge were studied. This stratigraphic constraint was lacking in previous studies—Meisel et al. (1990) are likely to have analyzed samples from the Florence Sandstone and the Bell Shale exposed by bulldozer during access track constructions. The position of analyzed core samples is depicted in Fig. 5.

Outcropping suspected target rock samples were carefully selected to avoid analyses of highly weathered samples. These hand-sized specimens were split into ~10 mm chips and the weathered material was discarded. The chips were further crushed using a hydraulic crusher and cleaned of dust with an air hose. In analyses that exclude Co, around 40 g of the crushed material was ground in the tungsten carbide ring mill. For most analyses that include Co, the crushed material was further pulverized in an agate mortar and pestle before being further crushed to fine powder in an agate ring mill.

X-Ray Fluorescence (XRF) Analyses

Fusion discs of the powdered target rock samples were prepared for determining the major elements (SiO₂, Al₂O₃, TiO₂, MnO, MgO, FeO, K₂O, CaO, Na₂O, P₂O₅) by X-ray fluorescence (XRF). Pressed pills were used for XRF analysis of the following trace elements: Cr, Co, Ni, Cu, Zn, Ga, Nb,

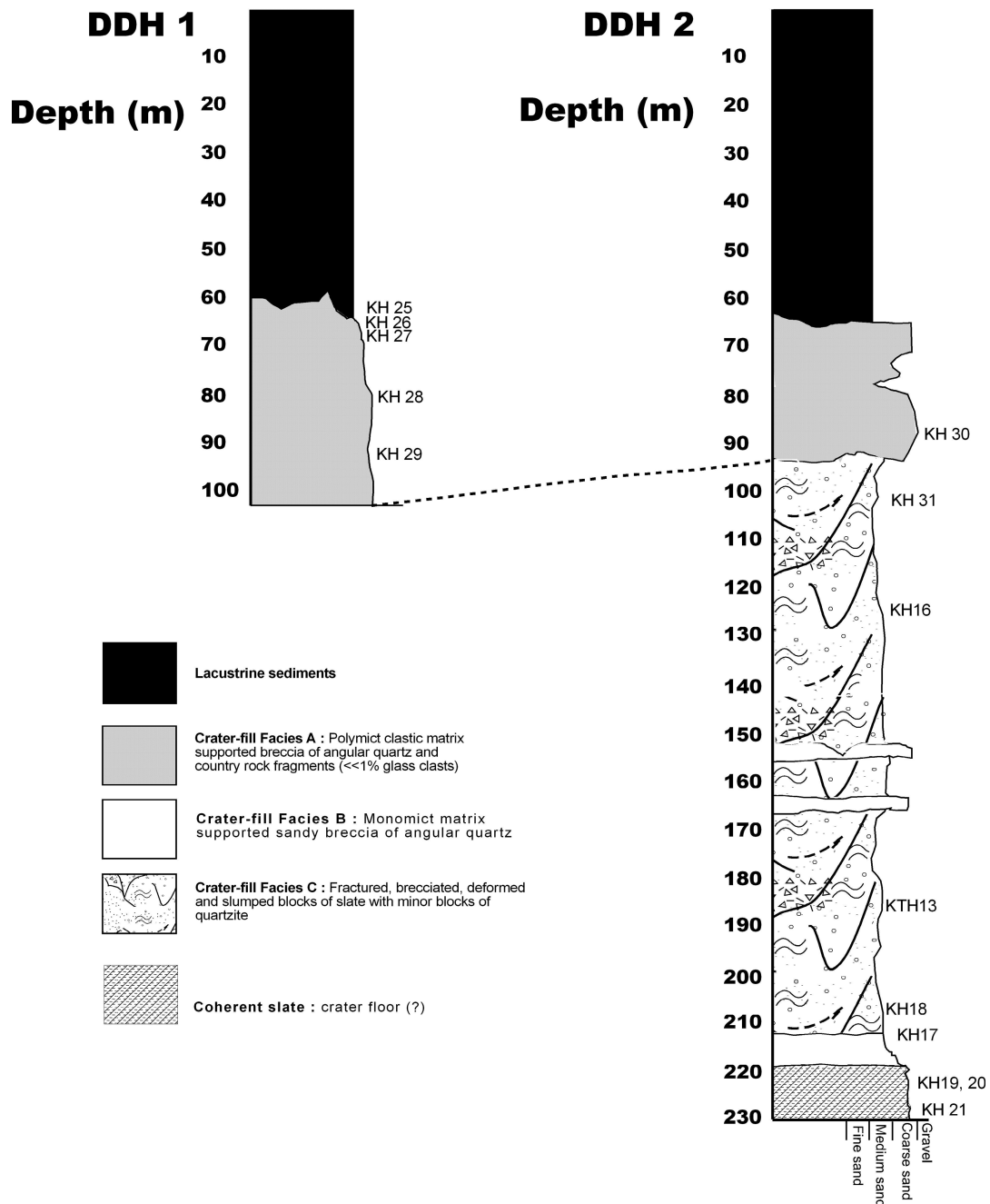


Fig. 5. Darwin crater drill core stratigraphy. The location of samples selected for geochemical analyses are indicated.

Rb, Sr, Ba, Zr, and Y. These analyses were conducted on an automated Phillips PW 1480 XRF spectrometer at the School of Earth Sciences, University of Tasmania. Mr. Phillip Robinson provided calibrations.

Solution ICPMS

Portions of samples (KH 1,2,4,6,7,8,12,15,17,18,19) that were analyzed by XRF were dissolved using HF and HNO₃ acids and brought to a 1:1000 dilution in 2% HNO₃ to allow

analyses using ICP-MS. This technique was chosen primarily to determine the REE geochemistry of the suspected target rocks, but trace elements determined by XRF were also analyzed by ICPMS and it is these that are reported here. The following trace elements were determined: Sc, Cr, Co, Ni, Ga, Rb, Sr, Y, Nb, Sb, Cs, La, Ce, Pr, Nd, Sm, Eu, Gd, Tb, Dy, Ho, Er, Yb, Lu, Hf, Ta, Pb, Th, and U. The abundance of the trace elements in these samples was calibrated against the rock standard BHVO-1. Instrument drift was monitored and corrected using La and Ti as internal standards.

Table 1. Major-element composition of Darwin glass.

	Site	SiO ₂	Al ₂ O ₃	TiO ₂	FeO	MgO	CaO	K ₂ O	Na ₂ O	n
Macro-glass		76.47–93.85	3.14–11.45	0.22–0.8	0.84–5.87	0.24–4	0.02–0.25	0.75–2.71	0–0.21	
	Average	84.6	7.52	0.58	2.55	1.13	0.06	1.87	0.1	216
Mini-glass		75.24–93.18	1.98–10.68	0.13–0.7	0.74–6.2	0.19–3.67	0–0.22	0.61–2.4	0.02–0.19	
	Average	84.41	7.37	0.56	2.87	1.56	0.09	1.71	0.08	78
Meisel et al. (1990)		84–89.3	6.75–8.20	0.52–0.62	1.08–3.78	0.61–1.13	0.03–0.18	1.51–2.93	0.02–0.06	18
Taylor and Solomon (1962)		84.1–87.1	5.8–7.44	0.56–0.62	1.44–2.98	0.66–1.36	0.05–0.19	1.66–1.98	0.03–0.07	10

Analyses by SEM; detection limits are between 0.05–0.1 wt%.

Isotopic Analyses

Rb-Sr and Sm-Nd isotope systematics were studied in 12 samples: three slates (Amber Slate); three quartzites (Keel Quartzite); three crater-fill samples (Fig. 5) and three pieces of glass. The analyzed slates and quartzites samples were collected proximal to the crater; isotope abundances were not determined for Crotty quartzite owing to the lack of such a stratigraphically constrained sample from close to the crater. Rb, Sr, Sm, and Nd concentrations and isotope compositions were determined by Dr. Karin Barovich at the University of Adelaide. Sr and Nd isotopic compositions were measured in static mode on a Finnigan MAT 262 thermal ionization mass spectrometer. The average ⁸⁷Sr/⁸⁶Sr ratio for standard NIST SRM987 during the course of the study was 0.710264 ± 28 (2 σ) on 12 runs. The procedural blanks for Sr are better than 1 ng. Whole rock powders were dissolved and split before spiking with ⁸⁴Sr and ⁸⁵Rb. Samples for the Sm-Nd analyses were spiked with a mixed ¹⁴⁹Sm-¹⁵⁰Nd spike. The value for standard Lajolla gave a ¹⁴³Nd/¹⁴⁴Nd ratio of 0.511848 ± 8 (2 σ). The procedural blanks for Nd are less than 300 pg and for Sm less than 150 pg.

RESULTS

Major Elements in Darwin Glass

The ranges in composition for the major elements in the analyzed macro Darwin glasses are: SiO₂ (76.5–93.9%), Al₂O₃ (3.1–11.4%), TiO₂ (0.2–0.8%), FeO (0.8–5.9%), MgO (0.25–4.0%), K₂O (0.7–2.7%), CaO (<0.01–0.3%), and Na₂O (<.01–0.2%). For the analyzed mini-glasses, the ranges in major-element composition are: SiO₂ (75.24–93.18%), Al₂O₃ (1.98–10.68%), TiO₂ (0.13–0.7%), FeO (0.74–6.8%), MgO (0.19–3.67%), K₂O (0.61–2.4%), CaO (<0.01–0.22%), and Na₂O (<.01–0.19%). A summary of the mean and range in the major-element composition of Darwin glass is presented in Table 1. Macro and mini Darwin glasses have overlapping ranges in major-element compositions and very similar average compositions, however, relative to average macro Darwin glass, the average mini-glass is slightly enriched in MgO (+0.46%)

and FeO (+0.27%) and depleted in K₂O (–0.2%). This variation is insufficient to define the mini-glasses as geochemically distinct from the macro glasses. On the basis of major-element geochemistry, all of the analyzed samples are considered to be parts of the same population. These mean results are similar to previously published analyses of Darwin glass (e.g., Taylor and Solomon 1962; Meisel et al. 1990). However, average Darwin glass in this study is depleted in SiO₂ and enriched in MgO relative to previous studies. This study extends the ranges in composition of Darwin glass for all analyzed major elements.

Trace Elements in Darwin Glass

A summary of the mean and range of trace element abundances in macro and mini Darwin glasses is presented in Table 2. All of the glasses show affinity with upper crustal sediments and are relatively enriched in light REE (LREE) (La/Lu = 5.9–10) with pronounced negative Eu anomalies (Eu/Eu* = 0.55–0.65). Macro and mini Darwin glasses have overlapping compositional ranges and very close average compositions for all elements except Cr, Co, and Ni that are enriched in the mini-glasses. With the exception of Ni (enriched by >30%), the results are within 20% of previously published analyses (e.g., Meisel et al. 1990). These data extend the previously reported compositional ranges for the trace elements in Darwin glass. The variation in trace element compositions in Darwin glass is strongly affected by SiO₂ closure. This artefact produces a statistically significant negative correlation between SiO₂ and all trace elements.

A cluster analysis performed on the following major- and trace-element data: Na₂O, MgO, Al₂O₃, SiO₂, K₂O, CaO, TiO₂, FeO, Sc, Cr, Co, Ni, Rb, Sr, Zr, and Ba resulted in a dendrogram with two main compositional groups (Table 3). Group 1 includes 80% of the sample and is characterized by large variations in major-element compositions. In hand samples and thin sections, glasses belonging to group 1 are predominantly white to dark green in colour. The range in major-element composition in group 1 glass is: SiO₂ (80.62–93.9%), Al₂O₃ (3.14–10.6%), TiO₂ (0.2–0.76%), FeO (0.8–4.23%), MgO (0.25–2.31%), and K₂O (0.7–2.7%). The average composition

Table 2. Trace element composition of Darwin glass.

	Macro-glasses		Mini-glasses		Meisel et al. (1990)	Taylor and Solomon (1962)
	Range (ppm)	Average (ppm)	Range (ppm)	Average (ppm)	Range (ppm)	Range (ppm)
Cs	1.5–5.8	3.8	1.6–6.7	3.3	2.5–4.5	3.2–4.3
Rb	33.3–109.3	75.3	35.5–118.1	67.7	71–137	61–110
U	0.6–4	1.9	0.4–3.6	1.5	1.5–5.4	–
Th	4.5–22.8	14	6.6–18.8	13.9	12–19	–
Ba	116.7–457.2	304.9	166.8–384.7	293.5	182–450	290–360
La	48.9–11.3	36.2	17.1–45.5	35.1	35–46.5	–
Ce	26.9–110.3	79.4	41.2–105.2	78.3	70–97.8	–
Nb	4.6–16	11.6	6.0–14.6	11.2	–	–
Pr	2.7–12.5	8.7	4.4–11.3	8.5	–	–
Sr	4.9–27.8	15.6	7.9–24.3	14.8	–	13–16
Nd	10.7–48.2	33.4	16.1–43.4	32.2	29–42	–
Zr	54.1–50.9	433.2	180.6–919.6	416.7	254–547	220–490
Sm	2.1–10.7	6.9	3.4–8.6	6.7	6.6–9	–
Eu	0.4–1.9	1.3	0.7–1.8	1.3	0.9–1.5	–
Gd	1.9–11.1	6.6	3.3–8.2	6.2	–	–
Ho	0.3–2.0	1.2	0.6–1.7	1.2	–	–
Yb	0.8–4.9	3.3	1.3–4.4	3.1	2.7–4.5	–
Y	7.4–53.4	34.1	14.2–45.4	31.9	–	18–44
Lu	0.1–0.8	0.5	0.1–0.6	0.5	0.1–0.8	–
Sc	3.5–10.8	7.3	3.9–9.8	6.8	6–8.2	2.5–5.2
Cr	19.5–505.2	89.9	39.4–371.7	120.2	48–522	69–205
Co	0.3–56.7	12.7	4.2–59.7	20.4	4.6–39	<3–27
Ni	3.0–917.7	161.3	34.7–841.8	246.2	30–536	82–205

Analyses by LA-ICPMS; detection limits between 0.1 and 0.0001 ppm.

of group 1 glass is close to that of bulk average Darwin glass. The second population identified in the cluster analysis is characterized by a narrower range in and lower average abundance of SiO₂ (76.5 to 84.1%, with an average of 81.2%). In hand samples and thin sections, group 2 glass is almost always black. The average MgO (2.2%) and FeO (3.8%) compositions of group 2 are significantly higher than those of group 1 glass or average Darwin glass, and Al₂O₃ is also slightly enriched. The average Cr (162 ppm), Co (31 ppm), and Ni (416 ppm) content of group 2 glass is also significantly enriched relative to group 1 glass or average Darwin glass, with the remaining trace elements being of very similar abundance in both groups. On the basis of 18 samples, Meisel et al. (1990) identified 3 chemically distinct glass groups and importantly one sub-population enriched in Mg and the transition metals was identified. Taylor and Solomon (1962) also reported anomalous enrichments in Ni, Co, and Cr in some Darwin glasses.

Major Elements in Suspected Target Rocks and Crater-Fill Samples from Darwin Crater

Analyses of surface Eldon Group rocks and crater-fill samples from the drill cores are presented in Table 4. The average SiO₂ content is highest in the surface samples of Crotty (94.6%) and Keel (90.09%) Quartzite, followed by

Amber Slate (75.41%). For most major elements, the deformed rocks from the drill core show obvious affinity with the Amber Slate and Keel Quartzite (KH17) cropping out around the crater. In some samples the effects of weathering on the crater-fill are obvious. For example, in sample KH19 (taken from a highly fractured and brecciated zone filled by the oxyhydroxide goethite), the FeO content reaches 33.5% at just 37% SiO₂. The polymict, allogenic breccia samples (crater-fill facies A) also show strong geochemical affinity with outcropping surface rocks and the deformed shales intersected in the drill cores, except for up to 5% S in samples KH25 and KH26 from the top of this facies. This elevated S content is consistent with petrographic observations and XRD data that indicate the secondary mineral Rosenite (Howard and Haines 2007).

Trace Elements in Suspected Target Rocks and Crater-Fill Samples from Darwin Crater

The range and average abundance of trace elements in surface and crater-fill samples from Darwin crater are presented in Table 5. For most elements, the slates show the most limited compositional range. In all analyses the REE—especially the LREE—show the least variation and range from between <2% (e.g., Sm in Amber Slate) and 60% (e.g., Gd in Keel Quartzite) of mean values. The transition metals Ni and Co and the alkaline

Table 3. Cluster analysis group classification of Darwin glass compositions.

Group	Na ₂ O	MgO	Al ₂ O ₃	SiO ₂	K ₂ O	CaO	TiO ₂	FeO	Sc	Cr	Co	Ni	Rb	Sr	Zr	Ba
Average group 1	0.05	0.9	7.3	85.2	1.8	0.05	0.05	2.2	7.2	74.5	8.7	108.4	74.6	15.8	438.9	304.3
Range	0.0-0.2	0.2-2.3	3.1-10.6	80.62-93.9	0.75-2.6	0.0-0.1	0.2-0.7	0.8-4.23	3.4-10.1	19.5-204.6	0.0-33.9	3.0-492.8	33.2-109.2	4.9-27.8	54.1-750.9	116.7-457.1
Average group 2	0.1	2.2	8.2	81.6	2	0.1	0.6	3.8	8.1	162.7	31.6	416.6	78.1	14.3	439	294
Range	0.0-0.2	1.1-4.0	6.4-11.5	76.4-84.5	1.4-2.7	0.06-0.2	0.5-0.80	1.8-5.8	6.3-10.7	67.6-260.4	19.4-56.5	117.4-917.7	56.6-109.2	10.9-20.4	286.6-553.1	210.7-427.3
Bulk average Darwin glass	0.1	1.1	7.5	84.6	1.9	0.1	0.6	2.6	7.3	89.9	12.7	161.3	75.3	15.6	433.2	304.9

The cluster analysis results in a dendrogram with 2 compositional groups. Group 1 is characterized by a wide range in SiO₂ abundance and a large degree of heterogeneity. Average group 1 glass is close in composition to bulk average Darwin glass. Group 2 glass has a more limited compositional range and a lower average SiO₂ abundance with significantly higher FeO and MgO contents. Group 2 is also enriched in Ni, Co, and Cr relative to group 1 and bulk average glass.

Table 4. Major-element composition of target rocks and crater-fill facies.

	Keel Quartzite		Amber Slate		Crotty Quartzite		Crater-fill facies B and C (Deformed slate and quartzite)		Crater-fill facies A (Polymict breccia)	
	Average	Range	Average	Range	Average	Range	Average	Range	Average	Range
SiO ₂	90.09	85.63-92.63	75.41	70.14-79.05	94.60	93.24-97.6	70.54	53.38-72.81	74.75	71.1-76.91
Al ₂ O ₃	5.43	4.13-8.44	11.83	10.29-14.6	2.82	1.11-3.94	11.32	4.43-9.26	9.55	4.95-12.6
TiO ₂	0.49	0.47-0.56	0.71	0.56-0.86	0.24	0.14-0.36	0.68	0.53-0.84	0.6	0.36-0.78
FeO	0.42	0.31-0.62	3.28	1.88-4.57	0.35	0.22-0.59	6.18	1.6-10.75	4.03	2.07-6.88
MgO	0.35	0.27-0.51	0.01	0.01-1.58	0.15	0.09-0.17	0.97	0.32-1.53	0.96	0.52-1.28
MnO	0.01		<0.01	<0.01-0.02	<0.01		0.19	<0.01-1.01	0.03	<0.01-0.21
CaO	0.08	0.01-0.29	0.08	0.01-0.32	0.07	0.01-0.15	0.27	0.05-1	0.66	0.06-2.44
K ₂ O	1.82	1.44-2.81	3.47	2.92-4.04	0.99	0.38-1.24	3.2	1.11-4.69	2.79	1.43-3.79
Na ₂ O	0.03	0.01-0.05	0.20	0.11-0.42	0.02	0.0015-0.0	0.09	<0.03-0.14	0.09	0.06-0.14
P ₂ O ₅	0.07	0.01-0.3	0.14	0.1-0.35	0.70	0.01-0.7	0.19	0.037-0.46	0.12	0.01-0.3
n	6		8		4		8		5	

Determined by XRF.

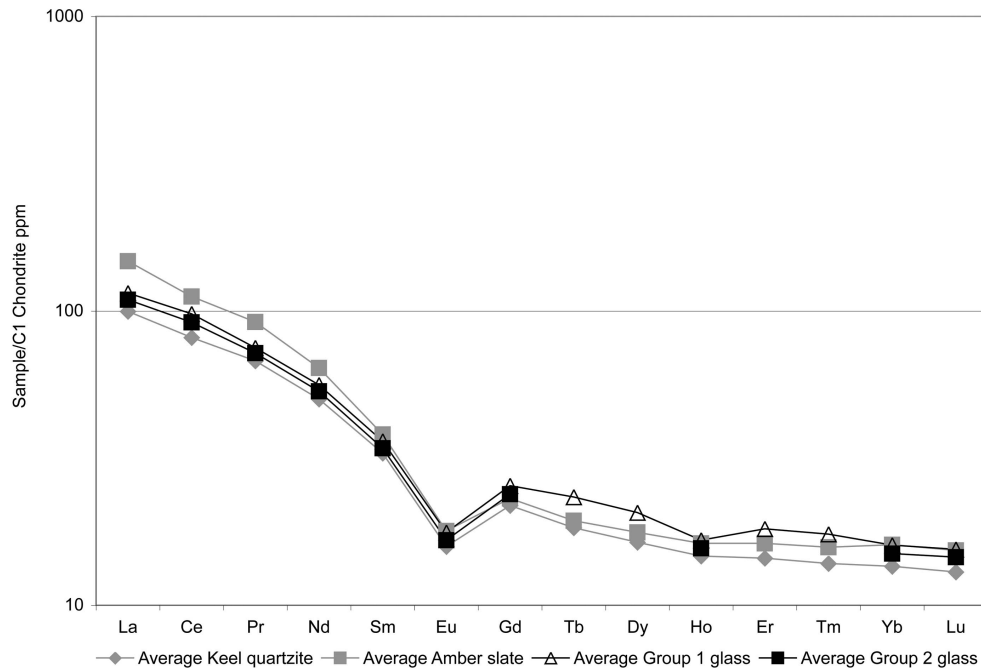


Fig. 6. Chondrite normalized REE composition of Darwin glass, target rocks, and crater-fill samples. Chondrite values from Sun and McDonough (1989).

earth Sr show the greatest compositional ranges of the determined elements. This large variation in analytical results—particularly for the transition metals—relates to the dilution effect of quartz and the subsequent very low abundance of these elements in the most quartz-rich samples. The ranges in the abundance of all trace elements in the crater-fill samples fall largely within the total ranges for the analyzed Eldon Group rocks from around the crater. The obvious exceptions being enrichments in heavy REE (HREE) plus Y, transition metals Ni, Co, Cr and the sulfide metals Zn, As, Cu, and Pb in crater-fill facies C. This enrichment is interpreted to be related to weathering processes and is most pronounced in those analyzed samples with the most abundant Fe-oxyhydroxides such as KH19 that has up to 150 ppm Ni, 190 ppm Cr, and 720 ppm Y!

GLASS VERSUS TARGET

Major and Trace Element Data

A comparison of the composition of Darwin glass and target rocks from Darwin crater shows:

- Major elements in group 1 Darwin glass are closest to average Keel Quartzite (Sk) but are dramatically enriched in FeO and also enriched in MgO, P₂O₅, and SiO₂ relative to the quartzite. In group 1 glass, all major elements other than SiO₂ are depleted compared to average Amber Slate (Sa). Group 1 glass is enriched in all elements other than SiO₂, MgO, CaO and P₂O₅ relative to average Crotty Quartzite (Sc). Group 2 glass is most similar in major-element composition to Amber Slate.

- The glasses are very slightly depleted in LREE relative to average Amber Slate and very slightly enriched in La and Ce relative to average Keel Quartzite. The remaining LREE abundances are effectively identical in both Darwin glass and Keel Quartzite. For the other HREEs and Y, the glasses and suspected target rocks have overlapping abundances similarly shaped patterns (Fig. 6).
- For the alkali metals, the alkali earth Ba, and actinide elements, the glass compositions overlap the target rocks and are closest to average Keel Quartzite (Fig. 7).
- The average Zr abundances in the glass falls within the range in Zr abundances of the suspected target rocks (Fig. 7).
- Average Rb/Sr in group 1 (4.8) and 2 (5.2) glasses falls within the compositional range defined by average Crotty Quartzite (3.55), Keel Quartzite (7.17) and Amber Slate (9.98). The strongly depleted concentration of Sr and high Rb/Sr ratios in both the glass and suspected target rocks, relative to average crustal rocks, is the key feature of the non-transition metal trace element chemistry that links the glass to these target rocks.
- The upper limits in the abundance of Ni, Co, and Cr in group 2 Darwin glass samples are more than 20, 6, and 2 times the average suspected target rock values, respectively.

Isotope Data

Results of isotopic analyses (Table 6) show:

Table 5. Trace element composition of target rocks and crater-fill facies.

	Keel Quartzite		Amber Slate		Crotty Quartzite		Crater-fill facies B and C (Deformed slate and quartzite)		Crater-fill facies A (Polymict breccia)		KH19	KH29
	Average	Range	Average	Range	Average	Range	Average	Range	Average	Range		
Cs	4.27	4.12–5.51	9.69	7.71–12.35	36.13	14.6–45.6	9.50	3.98–13.92	123.70	68.9–158.7	9.65	13.80
Rb	62.85	14.6–110.5	161.24	128.2–197.7			147.80	49.7–197.3			83.40	
U	2.17	1.75–2.73	3.33	2.91–3.83			3.24	1.99–4.11			7.94	
Th	10.58	7.89–13.37	17.85	15.54–20.54			17.34	14.61–21.57			21.98	
Ba	232.52	108.9–350.5	562.01	503.7–707.3	124.52	108.9–143.97	459.43	181.8–627	428.48	248.3–578.7	371.80	56.50
La	31.33	29.77–34.19	46.45	43.84–49.44			41.66	33.91–51.38			87.42	
Ce	65.94	61.59–74.09	90.91	85.51–96			87.66	73.22–107.21			161.56	
Nb	8.83	4.1–12.5	16.36	13.8–19.83	5.23	4–8.1	15.65	10.55–20.2	13.44	8.2–17.8	10.74	1.50
Pr	7.85	7.19–8.96	10.64	9.96–11.12			10.40	8.57–12.9			22.32	
Sr	8.76	1.2–22.56	16.15	9–22.9	10.15	1.2–20.6	12.97	6.65–28.82	24.02	12.1–37.2	16.81	426.60
Nd	29.90	26.61–35.35	38.22	35.66–39.72			40.47	33.95–50.25			106.44	
Zr	309.82	112.9–600.3	336.79	222.6–404	171.24	112.9–305.5	319.99	254–440.8	290.14	236.1–345	265.10	33.40
Sm	6.31	4.96–8.67	7.31	6.81–7.63			9.09	7.87–11.16			36.26	
Eu	1.14	0.83–1.64	1.29	1.18–1.39			1.82	1.62–2.19			11.68	
Gd	5.64	4.01–8.42	5.96	5.65–6.25			8.65	7.46–10.84			69.06	
Ho	1.07	0.87–1.48	1.18	1.14–1.25			1.57	1.24–2.17			24.08	
Yb	2.82	2.26–3.91	3.34	3.18–3.6			4.06	3.31–5.86			81.88	
Y	24.19	9–39.67	31.39	26.2–35.8	15.63	9–21.2	52.17	33.19–85.8	41.40	19.7–63.5	859.83	23.30
Lu	0.42	0.34–0.58	0.50	0.47–0.53			0.60	0.44–0.88			13.71	
Sc	6.09	4.33–6.97	11.20	9.95–12.65			9.11	4.66–13.42			94.75	
Cr	54.52	37.3–57.1	85.39	72–100	80.83	76.34–87.1	90.64	44.7–119.9	75.72	55.4–85.5	190.30	8.20
Co	1.43	1–2.4	3.65	1–6.2	5.15	2.2–8.1	10.77	1–19.1	14.66	5.4–20.7	15.31	<2
Ni	7.42	0.5–12.3	21.53	9.2–29.1	4.35	0.5–9.7	42.76	7.6–93.5	30.54	15.6–43.2	153.93	5.70
n	6		8		4		8		5		1	1

Determined by XRF and solution ICP-MS.

Table 6. Rb-Sr and Sm-Nd elemental concentrations, isotope ratios, and Nd model ages for target rocks, crater-fill samples and Darwin glass.

Sample	Lithology	Sm (ppm)	Nd (ppm)	¹⁴⁷ Sm/ ¹⁴⁴ Nd	Error	¹⁴³ Nd/ ¹⁴⁴ Nd	Error	e—Nd	tCHUR (ma)	Rb (ppm)	Sr (ppm)	⁸⁷ Rb/ ⁸⁶ Sr	Error	⁸⁷ Sr/ ⁸⁶ Sr	Error
KH1	Keel Quartzite (Sk)	4.59	27.63	0.1	0.00	0.51	0.00	-15.70	1273.14	110.50	4.74	68.31	2.73	1.12	0.00
KH2	Keel Quartzite (Sk)	8.35	35.57	0.14	0.00	0.51	0.00	-13.58	1932.72	84.60	22.56	10.64	0.43	0.78	0.00
KH4	Keel Quartzite (Sk)	4.86	25.8	0.11	0.00	0.51	0.00	-15.17	1430.54	63.00	11.05	16.24	0.65	0.82	0.00
	Average	5.93	29.66	0.12	0.00	0.51	0.00	-14.82	1545.47	86.03	12.78	31.73	1.27	0.91	0.00
KH6	Amber Slate (Sa)	7.13	40.24	0.11	0.00	0.51	0.00	-15.64	1363.96	179.70	20.17	25.52	1.02	0.88	0.00
KH7	Amber Slate (Sa)	6.23	34.73	0.11	0.00	0.51	0.00	-15.86	1402.00	157.10	18.37	24.47	0.98	0.87	0.00
KH8	Amber Slate (Sa)	6.61	40.53	0.1	0.00	0.51	0.00	-15.59	1239.93	197.70	9.00	n.d	n.d	n.d	n.d
	Average	6.66	38.5	0.1	0.00	0.51	0.00	-15.70	1335.30	178.17	15.85	25.00	1.00	0.88	0.00
KH15	Crater-fill	7.58	36.29	0.13	0.00	0.51	0.00	-14.35	1586.81	96.20	28.82	9.45	0.38	0.76	0.00
KH17	Crater-fill	7.63	33.92	0.14	0.00	0.51	0.00	-13.57	1744.19	49.70	6.65	21.34	0.85	0.85	0.00
KH18	Crater-fill	9.32	48.16	0.12	0.00	0.51	0.00	-14.16	1386.29	171.80	7.49	n.d	n.d	n.d	n.d
	Average	8.18	39.46	0.13	0.00	0.51	0.00	-14.03	1572.43	105.90	14.32	15.39	0.62	0.81	0.00
KH22	Light green glass	7	34.91	0.12	0.00	0.51	0.00	-14.83	1533.57	74.90	12.60	16.90	0.68	0.81	0.00
KH23	Dark green glass	7.12	35.45	0.12	0.00	0.51	0.00	-14.54	1504.93	82.60	17.20	13.66	0.55	0.81	0.00
KH24	Black glass	6.74	34.82	0.12	0.00	0.51	0.00	-15.11	1478.66	82.90	17.60	13.41	0.54	0.82	0.00
	Average	6.95	35.06	0.12	0.00	0.51	0.00	-14.83	1505.72	80.13	15.80	14.66	0.59	0.81	0.00

Regression calculated in Excel using Isoplot. Errors are 2σ (4%).

- $^{87}\text{Sr}/^{86}\text{Sr}$ ratios for the glasses fall within the very large range (0.76481–1.1212) defined by all suspected target rocks and crater fill samples.
- The glass, suspected target rock, and crater-fill samples have homogeneous $\epsilon\text{-Nd}$ results ranging from –13.57–15.86 with the glasses falling close to the middle of this compositional range (–14.54–15.11; Fig. 8). Nd model (CHUR) ages for all analyzed samples range from 1.2–1.9 Ga using a reference chondritic mantle reservoir (CHUR) and the glasses (1.2–1.5 Ga) fall within the range defined by the suspected target and crater-fill samples.
- On isochrons the glass, suspected target rock, and crater-fill samples define linear trends with glasses falling near to the center of the data array in plots of both of $^{143}\text{Nd}/^{144}\text{Nd}$ versus $^{147}\text{Sm}/^{144}\text{Nd}$ and $^{87}\text{Sr}/^{86}\text{Sr}$ versus $^{87}\text{Rb}/^{86}\text{Sr}$ (Figs. 9a and 9b). A Rb–Sr regression line through all of the analyzed samples yields an age of 411 ± 42 Ma (2σ) and an initial $^{87}\text{Sr}/^{86}\text{Sr}$ value of 0.725 ± 0.016 (2σ). In the Sm–Nd system, the initial $^{143}\text{Nd}/^{144}\text{Nd}$ ratio is 0.51153 ± 0.00011 (2σ) and the regression yields an age of 451 ± 140 Ma (2σ). These age estimates overlap and are consistent with each other within the error limits of these data.

MIXING MODELS

To further test the compatibility of the analyzed rocks as parent materials of Darwin glass, a least squares regression model was created in Excel. The preferred model is a 3-component mixture of average suspected target rock compositions (Table 7). Relative to the bulk average abundances the worst model fits are (in order) Ni, Co, MgO, Cr, and FeO. For the remaining elements the model produces a good match using an average target rock mixture of 43% Amber Slate (Sa), 24% Keel Quartzite (Sk) and 30% Crotty Quartzite (Sc) (Table 7).

The average of all individual model results for group 1 and 2 glasses have been separated and are compiled in Table 7. As is expected for group 1 glasses, these results are almost identical to those for the model of bulk composition using an average suspected target rock mixture of 43% Sa, 27% Sk and 30% Sc. In group 2, the average model result was 66% Sa, 4% Sk, and 30% Sc. This mixture results in increased residual errors for (in order) Ni, Co, Rb, MgO Cr, and FeO. The concentrations of the remaining elements are successfully modelled. When soil (e.g., KH15) or weathered samples (e.g., KH19) more enriched in transition metals are added to the mixing models the residual errors in Ni, Co, Cr, MgO, and FeO are not improved (Table 7), even if soil or weathered material is allowed to contribute at an unrealistically large level to the mix.

DISCUSSION

With the exception of the transition metals in some group 2 glass, all of the geochemical and isotopic data presented are

consistent with the interpretation that Darwin glass can be formed from impact melting of the suspected target rocks. Meisel et al. (1990) could also not reconcile the transition metal composition of some Darwin glass samples with the lower abundances measured in their studies of suspected target rocks. However, Meisel et al. (1990) could also not reconcile the lower abundances of Na, K, Rb and Cs in the glass relative to their suspected target rocks and suggested selective volatilization of these elements during impact. Based on data presented in this study, the evidence for volatilisation is very limited. P_2O_5 is the only element that is depleted in average glasses relative to the target rocks. P is typically considered to be a refractory element so a volatility control on its abundance in the glass would be surprising. Rather, the apparent loss of P_2O_5 in average glass relative to the target rocks is likely to be an artefact that reflects the wide variability in sedimentary rock compositions, and uncertainties in determining the indigenous P_2O_5 contributions. Here, the average P_2O_5 abundances over the bulk rock melted to form the glass may have been significantly less than the average values determined for the target rocks. The natural variability in sedimentary rock compositions may also explain the lower abundances of Na, K, Rb and Cs in the glass relative to the target rocks found by Meisel et al. (1990). It also seems that the suspected target rocks in the Meisel et al. (1990) study may have been sampled from the Florence Sandstone and Bell Shale some 2 km from the crater during access track constructions.

Sm Nd Isotopes

The Sr and Nd isotopic composition and regression ages are an inherited signal in the glass and do not reflect the glass formation age or time of impact that is placed at 816 ± 7 ka (Loh et al. 2002). Being relatively “young,” the glass has not been significantly altered by water and shows no evidence of devitrification. Analysed samples all contain primary textural features such as flow banding, “hot break surfaces” and surface vesicles. As such, surface flows or groundwater springs are not considered to have imprinted a secondary isotopic signal on the glass. In the case of the Rb–Sr system, the initial Sr ratio (0.725 ± 0.016 [2σ]) resulting from the regression is close to, or within error of, the estimated value for Silurian seawater (0.70875) and is also close to the value for modern seawater. The regression age might be considered to reflect the depositional age of the sediments, as 411 Ma is very close to the Siluro-Devonian boundary. However, given the analytical errors, the Rb–Sr regression age is also within error of the age of the Tabberabberan Orogeny that commenced at around 395 Ma (Williams 1989) and this may have reset the system. The isotopic composition and regression ages in the samples may reflect a combination of a depositional age signal and the effects of the orogeny. However, this interpretation assumes that the Rb–Sr and Sm–Nd fractionation, as measured in the impact glasses, reflects processes that occurred during deposition or later diagenesis and deformation of the target

Table 7. Mixing model parameters and results.

	SiO ₂	TiO ₂	Al ₂ O ₃	FeO	MgO	K ₂ O	Cr	Co	Ni	Y	Rb	Zr	Sr	Ba
Model component compositions														
Average Amber Slate (Sa)	75.4	0.7	11.8	3.3	1.3	3.5	85.9	3.7	21.5	31.4	161.2	336.8	16.2	562.0
Average Keel Quartzite (Sk)	90.1	0.5	5.4	0.4	0.4	1.8	55.8	1.4	7.4	24.3	62.9	309.8	9.0	232.5
Average Crofty Quartzite (Sc)	94.6	0.2	2.8	0.3	0.1	1.0	80.0	5.2	4.4	15.6	36.1	171.2	10.2	124.5
Soil	53.5	0.5	9.2	10.2	0.7	1.9	84.0	19.1	33.7	36.2	96.2	254.0	30.7	403.2
KH19	37.9	0.4	7.5	33.5	0.6	2.1	190.3	15.2	150.6	729.6	83.4	265.1	21.7	371.8
Bulk average glass	84.6	0.6	7.5	2.5	1.1	1.9	89.7	12.6	159.3	33.9	75.5	431.1	15.6	304.9
Average group 1 glass	85.2	0.6	7.3	2.2	0.9	1.9	74.5	8.8	108.4	34.1	75.3	433.2	15.6	304.9
Average group 2 glass	81.6	0.6	8.2	3.8	2.2	2.0	160.7	30.4	405.9	32.3	74.8	391.9	14.3	292.6
Model mixture: Sa, Sk, Sc														
For bulk average glass														
Model result (residual error) in normal units	1.0	0.1	0.6	0.9	0.4	0.5	33.8	9.3	148.3	9.2	25.9	156.3	3.5	53.8
Residual error as % of average composition	1.2	10.6	7.9	36.3	39.7	25.9	37.6	72.8	91.9	26.9	34.4	36.1	22.2	17.6
For average group 1 glass in normal units	1.0	0.1	0.5	0.8	0.3	0.4	26.0	5.9	101.2	9.7	22.8	165.0	3.6	42.0
Model result (residual error) in normal units	85.5	0.6	6.8	2.3	0.8	1.7	69.4	8.2	110.1	36.0	66.2	457.4	16.4	238.0
Residual error as % of average composition	0.9	0.0	0.9	1.5	1.2	0.7	76.2	27.5	393.0	6.3	43.3	108.2	2.5	118.9
For average group 2 glass in normal units	1.1	5.8	13.5	65.3	164.1	42.1	109.9	336.3	357.1	17.6	65.4	23.7	15.4	50.0
Residual error as % of average composition	4.9	0.1	0.6	0.7	0.5	0.3	31.4	7.1	145.7	7.4	13.7	156.2	3.4	36.4
Model mixture: Sa, Sk, Sc, KH19														
For bulk average glass														
Model result (residual error) in normal units	5.8	12.2	7.9	25.6	46.2	13.4	34.9	55.8	90.3	21.6	18.1	36.1	21.9	11.9
Residual error as % of average composition	2.4	0.1	0.6	0.6	0.5	0.4	30.6	9.4	146.4	7.6	17.9	146.5	3.9	38.3
Model mixture: Sa, Sk, Sc, soil, KH19														
For bulk average glass														
Model result (residual error) in normal units	2.8	10.7	8.4	25.0	43.9	20.6	34.1	74.7	91.9	22.4	23.7	34.0	25.1	12.6
Residual error as % of average composition	0.3	0.1	0.6	0.6	0.5	0.4	31.1	9.5	146.3	9.7	17.2	149.9	4.1	37.1
Model mixture: Sa, Sk, Sc, soil, KH19														
For bulk average glass														
Model result (residual error) in normal units	0.3	12.0	8.5	22.8	44.1	19.5	34.6	75.2	91.8	28.5	22.8	34.8	26.3	12.2
Residual error as % of average composition														

Using the Solver function in Excel, the least squares model was used to find the best compositional match for every glass analysis with target rock mixtures. The model was run subject to the constraint that the percentage contributions from each target rock can not be negative.

Model result
(Proportion of each component mixed)
Sa 46.8% Sk 23.5% Sc 29.7%
Soil KH19

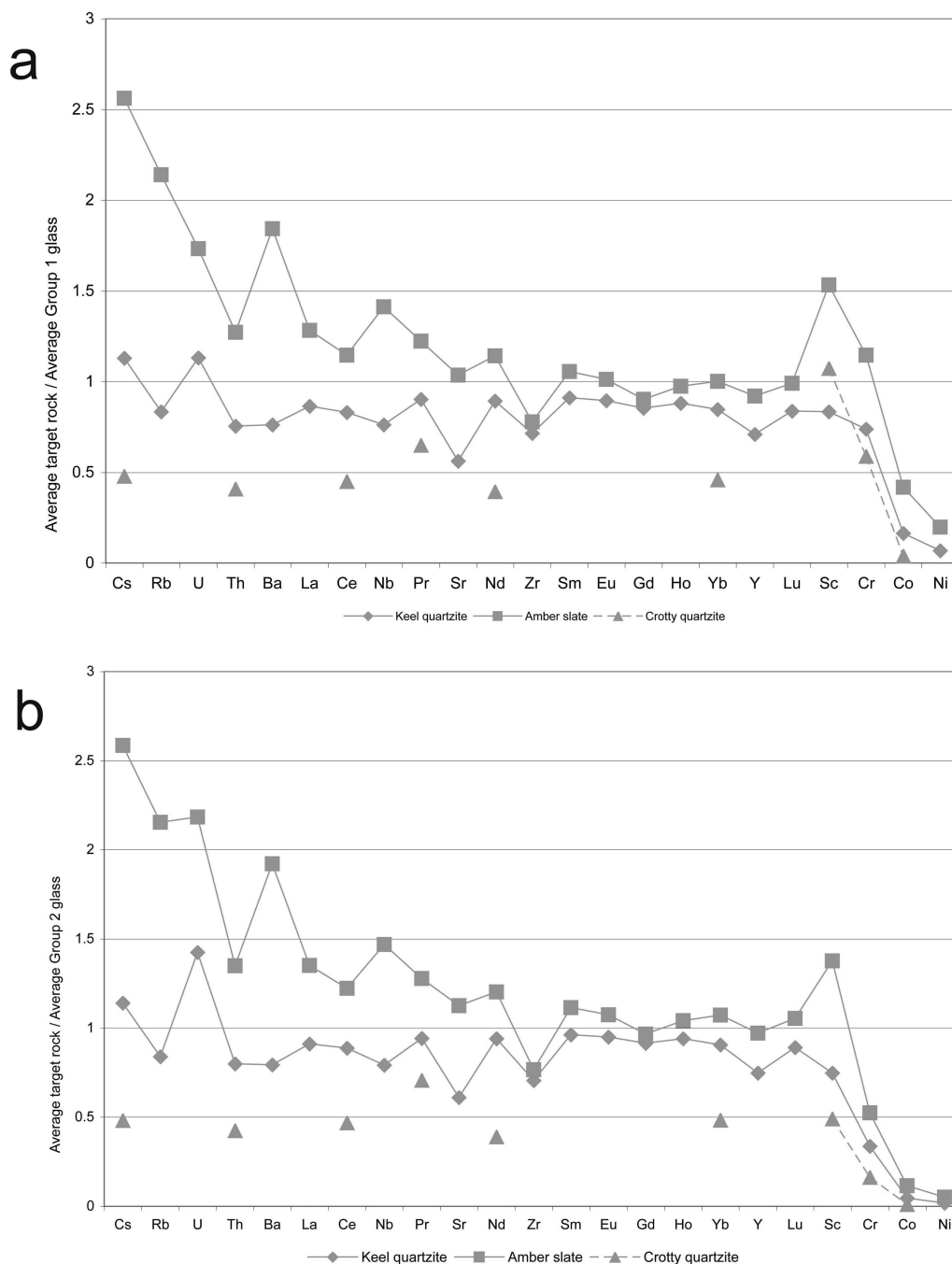


Fig. 7. a) Average target rock trace element compositions normalized to group 1 glass; b) normalized to group 2 glass.

rocks. The preferred interpretation is that the glass compositions reflect mixing and the isotopes are unlikely to have true age significance.

That these isotopic data support derivation of the glass from Eldon Group target rocks is particularly significant when other rock formations in the strewn field are considered. Volcanic and igneous rocks in the strewn field can be ruled out as potential targets on the basis of major and trace element glass geochemistry that indicates a sedimentary origin. Isotope data for the Mt. Read volcanics (MRV) in the center

of the strewn field also show distinctly different ϵ -Nd values than the glass or Eldon Group that range between +1 to -2 in basalts and andesites and $>+5$ in tholeiitic dykes (Whitford et al. 1990).

Data for non-Eldon Group sedimentary rocks in the strewn field are scarce. Raheim and Compston (1977) report Rb-Sr isotope data for a suite of Precambrian metasediments from near Strathgordon and the Collingwood River. These rocks are correlates of the Precambrian quartzites in the south of the strewn field. The initial Sr ratios in these rocks (average

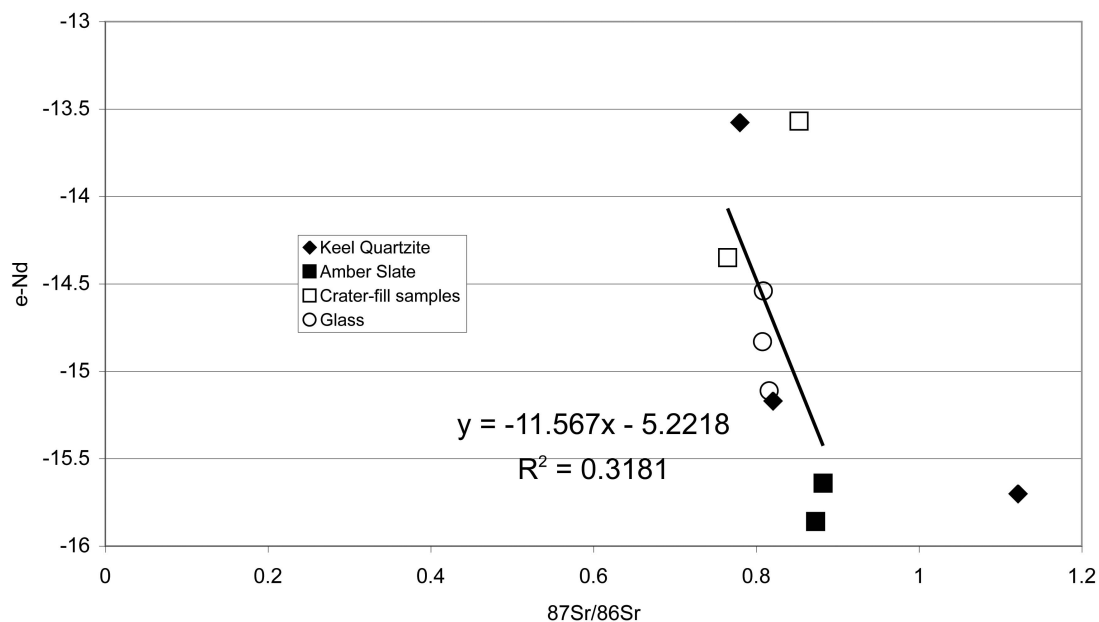


Fig. 8. ϵ -Nd versus $^{87}\text{Sr}/^{86}\text{Sr}$ in glass, target rocks and crater-fill samples.

Table 8. Selected major- and trace-element abundances in Tasmanian mafic and ultramafic rocks.

%	ppm							
	FeO*	MgO	Cr	Co	Ni	Ni/Co	Ni/Cr	Cr/Co
Average Tasmanian Jurassic dolerite (1)	8.8	6.6	108	30	78	2.6	0.7	3.6
Average Tasmanian west coast tholeiite (2)	11.9	7.1	261	30	133	4.4	0.5	8.7
Average Tasmanian lamprophyre (3)	12.2	15.0	480	75	430	5.7	0.9	6.4
Tasmanian west coast dunites (4, 5)								
Average	6.2	42.0	2084	100	2547	25.5	1.2	20.8
Maximum	7.8	49.5	2630	137	3090			
Minimum	5.5	33.3	1670	78	2072			
85-0135 median dunite	5.8	39.4	2010	100	2470	24.7	1.2	20.1
Tasmanian west coast pyroxenites (4, 5)								
Average	6.2	31.8	33	4839	70	10.2	0.1	70.9
Maximum	7.4	35.6	36	5770	85	903.0		
Minimum	4.3	21.0	30	3150	50	429.0		
85-0161 median pyroxenite	6.1	30.0	4836	76	540	7.1	0.1	63.6
Average group 1 Darwin glass	2.2	0.9	75	9	108	12.4	1.5	8.5
Average group 2 Darwin glass	3.8	2.2	161	30	406	13.4	2.5	5.3

*All iron as FeO. Data from (1) Hergt et al. (1989); (2) Crawford and Berry (1992); (3) Baillie and Sutherland (1992); (4) Brown (1986); Keays (personal communication in 2003).

0.72678 ± 0.00207) are within the range of the Eldon Group and glass, but regressions yield divergent data arrays and distinctly older model ages (Raheim and Compston 1977). The other significant sedimentary rocks in the strewn field belong to the Ordovician Denison Group. These siliceous conglomerates contain mostly Precambrian quartzite clasts and are expected to have significantly older Rb-Sr model ages than the suspected Eldon Group target rocks, but data are lacking. The Denison Group is not associated with any suspected impact structure and analyses suggest these conglomerates are too siliceous ($\text{SiO}_2 > 97\%$) to be the dominant target rocks involved in the formation of Darwin glass.

Explaining Cr, Co, Ni, MgO and FeO, Enrichments in Darwin Glass

The single aspect of the geochemical composition of Darwin glass that cannot be related to these suspected target rocks from Darwin crater is the transition metal (Co, Cr, Ni), MgO, and FeO concentrations in some group 2 glasses. Explaining these enrichments involves invoking an unknown mafic end-member. For comparison, analytical data for representative examples of west coast mafic and ultramafic rocks have been compiled in Table 8. Average Amber Slate is taken to represent the Ni, Co, and Cr contributed to the glass

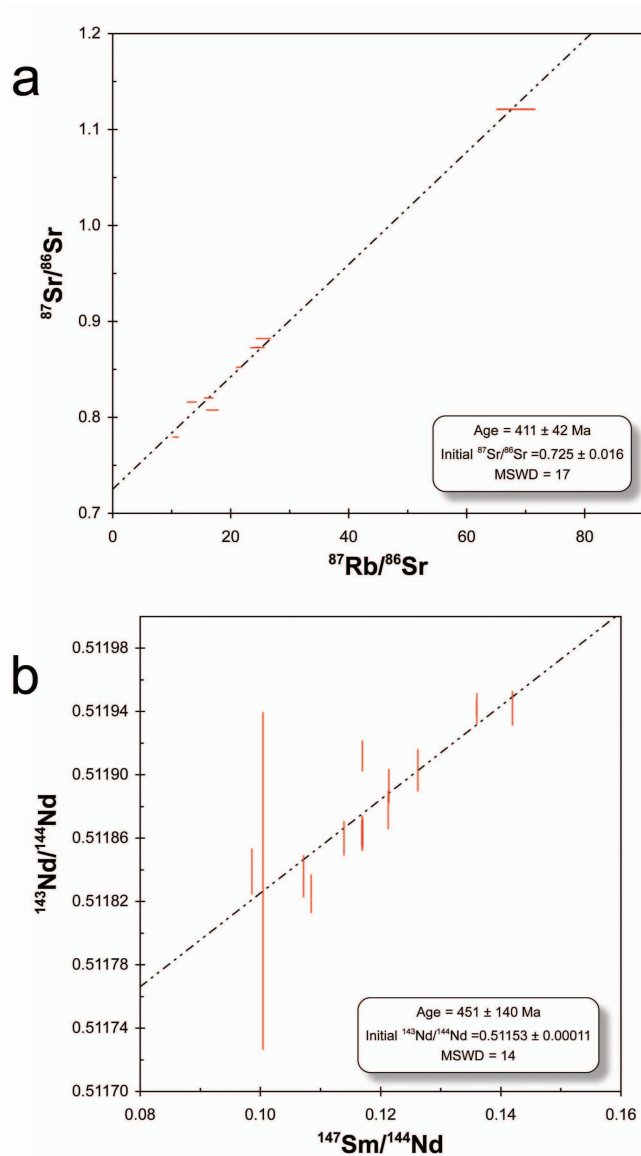


Fig. 9. a.) Rb-Sr isotopic evolution diagram for glass, target rocks, and crater-fill samples. Data point error ellipses are 2σ . b) Sm-Nd isotopic evolution diagram for identical samples as in Fig. 9a. Data point error ellipses are 2σ .

by the suspected target rocks, and linear mixing lines have been calculated between mixtures of slate and ultramafic rocks for Ni/Co, Ni/Cr and Cr/Co versus MgO (Figs. 10a–c) and FeO (Figs. 10 d–f). From these plots it is clear that at any given MgO or FeO content, Ni/Cr ratios in all of the volcanic rocks are lower than those found in the most enriched glasses. The mixing line with Amber Slate indicates that even a 100% contribution from the most Ni-rich rock, average dunite (Ni/Cr = 1.2), could not produce Ni/Cr ratios as high as in most group 2 glasses (average = 3.4) and as such the addition of FeO to the average Amber Slate or mixing with highly weathered samples like KH19 does not improve the model fit.

Ni/Co ratios in dunite and Darwin glass show better agreement and in the Ni/Co versus MgO plot, the mixing line between average Amber Slate and dunite passes through the group 2 glasses at up to about 10% contribution from dunite. However, these worst modelled glass compositions have excess FeO relative to average dunite at similar Ni/Co ratios. At any given FeO or MgO content, Ni/Co ratios in rocks other than the dunite (2.6–7.1) remain lower than for all group 2 glasses (average 13.4).

The dunite and pyroxenite have excess Cr relative to Co when compared to all of the glasses, and trends toward higher FeO and MgO defined by the mixing lines between these rocks and Amber Slate, are divergent from the glass arrays. On the Cr/Co plots, mixing lines between Amber Slate and average basalt, dolerite and ultramafic lamprophyre define trends in the broad direction of the most enriched glasses. However, at the required FeO and MgO abundances, the dolerite, basalt, and lamprophyre also have excess Cr relative to Co. Even if allowed to contribute an unrealistically large proportion to the melt, the mixing lines show that 100% contribution from the dolerite, basalt, or lamprophyres results in excess FeO and MgO, and Cr/Co ratios would be higher than for all group 2 glass samples. Significant to note is that based on limited analyses, Tasmanian West Coast lamprophyres (Cr/Co = >15; Baillie and Sutherland 1992) appear to be more differentiated than the plotted average ultramafic lamprophyres (Cr/Co <10, Rock 1991), which can be compared to an average Cr/Co ratio of 4.7 in the most enriched glasses. This makes any contribution from lamprophyres, which are the most geologically reasonable ultramafic candidates to exist in the target stratigraphy, even less likely.

As such, on the basis of excess Cr relative to Ni and Co it is not possible to mix west coast mafic or ultramafic rocks and Amber Slate, or any other analyzed suspected target rock, or multiple combinations thereof, to reproduce the Ni, Co, Cr, and MgO composition of the anomalous group 2 glass. Therefore, potential terrestrial sources of the enriched transition metals in these glasses, known from the west coast of Tasmania, can largely be excluded from any further consideration. The clear implication is that these anomalous enrichments may be related to the impacting projectile and it is perhaps significant that the transition metals show chondritic ratios in the most anomalous glass samples and this has previously been reported (Howard 2003). However, there is currently no evidence for Ir-enrichment in the glass that may be expected from any putative projectile. Meisel et al. (1990) also noted that a chondritic contribution may partly explain the composition of the most transition-metal-enriched glasses, but they too could not reconcile this with the absence of any apparent Ir enrichment and suggested an unknown ultra-basic unit in the target stratigraphy might be a better explanation. This

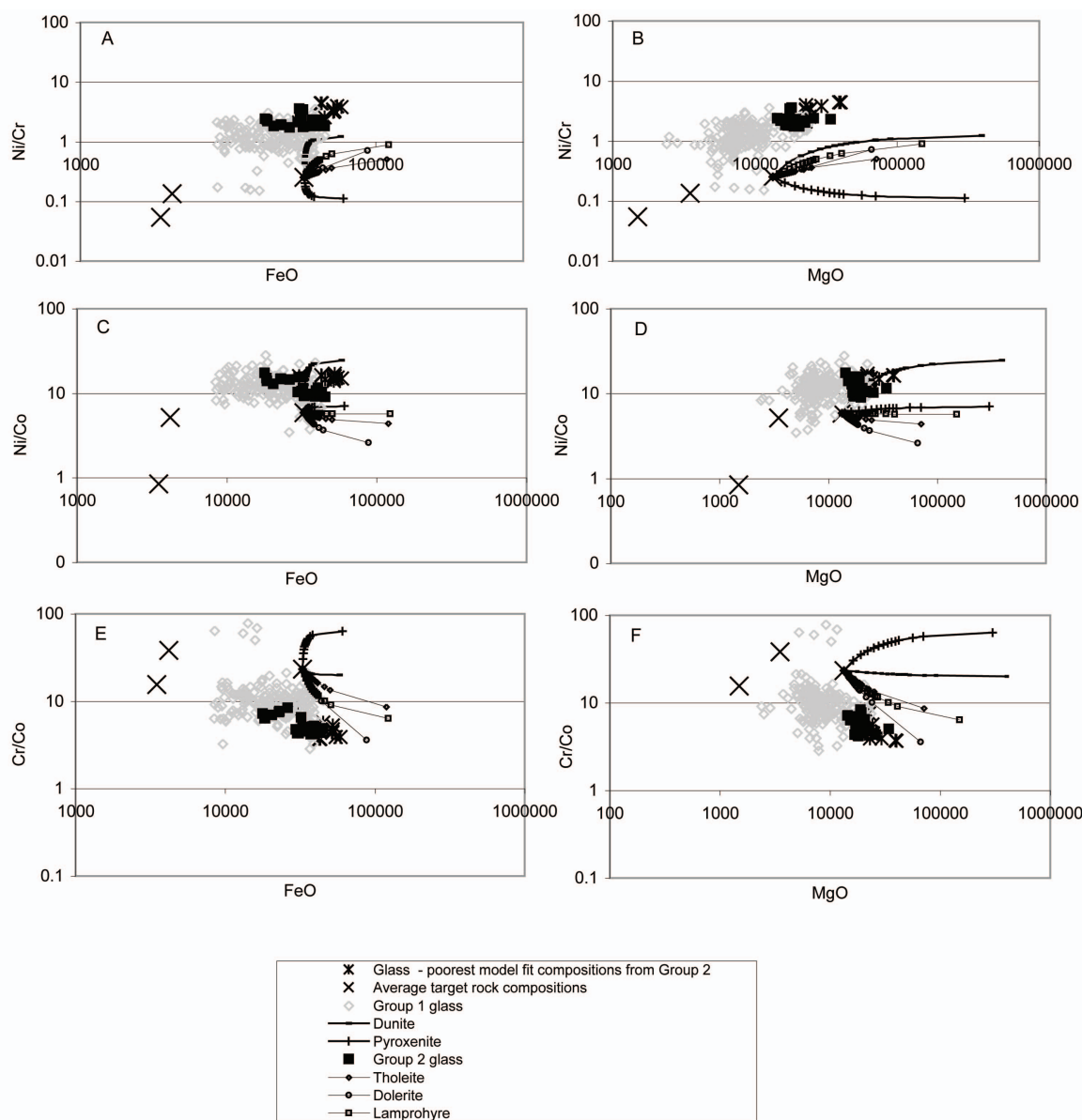


Fig. 10. a–f. Plots showing selected transition metal ratios versus MgO and FeO in Darwin glass, target rocks, and ultramafic rocks from western Tasmania. In each plot, linear mixing lines have been calculated between average Amber Slate and the ultramafic rocks in an attempt to model the composition of the most anomalous (high MgO, FeO, Ni, Cr, Co) glasses. The composition of the most transition-metal-enriched glass cannot be explained by a contribution from these ultramafic rocks. Data from Brown (1986), Keays (personal communication in 2003), Crawford and Berry (1992), Hergt et al. (1989), Baillie and Sutherland (1992).

study has shown that contributions from known terrestrial mafic and ultramafic sources in Tasmania fail to explain the composition of the most enriched group 2 glasses.

CONCLUSION

Data presented in this study show:

- Two compositional groups of glass: group 1: SiO₂ (80.62–93.9%), Al₂O₃ (3.14–10.6%), TiO₂ (0.2–0.76%), FeO (0.8–4.23%), MgO (0.25–2.31%), K₂O (0.7–2.7%);

group 2: SiO₂ (76.4–84.5), Al₂O₃ (6.4–11.5), TiO₂ (0.5–0.80), FeO (1.8–5.8), MgO (1.1–4.0), K₂O (1.4–2.7). group 2 glass is also significantly enriched in Ni (117.4–917.7), Co (19.4–56.5), and Cr (67.6–260.4) relative to group 1 or bulk average Darwin glass and all of the target rocks.

- Major elements in the high SiO₂ group 1 Darwin glass samples are closest to Keel Quartzite and major elements in the low SiO₂ group 2 glasses are more similar to Amber Slate.

- Trace elements in the glasses show affinity with both Keel Quartzite (Ba, actinides, LREE) and Amber Slate (Sr, HREE plus Y), suggesting that the glass groups represent mixtures of the shale and quartzite.
- The glasses and suspected target rocks have concordant REE abundance patterns typical of upper crustal sediments.
- Sr and Nd isotope data indicate that the glasses have an inherited isotopic composition consistent with formation from a mixture of the suspected target rocks.
- Mixing calculations using average Eldon Group compositions successfully model the glass composition. Such models result in significant errors only for Ni, Co, MgO, Cr, and FeO in some anomalous group 2 glass samples.

Therefore, the geochemical and isotopic systematics in rocks at Darwin crater are consistent with these rocks being the source materials melted under impact conditions to produce Darwin glass. The huge compositional heterogeneity in Darwin glass indicates that this mixing of molten target rocks was incomplete and that the melt quenched rapidly. Transition-metal-enriched group 2 glasses require an ultramafic contribution. However, mixing models with dunites, pyroxenites or lamprophyres fail to produce the required glass compositions and these rock types are not present in the target rock stratigraphy. The implication is that these transition metal-enriched glasses are preserving the geochemical signature of the impacting projectile.

Acknowledgments—Peter Haines, Ron Berry, Clive Burrett, and Marc Norman provided valued insights. Parts of this research were funded by the Barringer Family Fund for Meteorite Impact Research Award received by the author in 2003. Two anonymous reviewers are thanked for their constructive comments. The Tasmanian Aboriginal people are the traditional owners of Darwin glass.

Editorial Handling—Dr. John Spray

REFERENCES

- Baillie P. W. and Sutherland F. L. 1992. Devonian lamprophyres from Mt. Lyell, western Tasmania. *Papers and Proceedings of the Royal Society of Tasmania* 126:19–22.
- Brown A. V. 1986. Geology of the Dundas-Mt. Lindsay-Mt. Youngback region. Tasmania Department of Mines. *Geological Survey Bulletin No. 62*. 218 p.
- Corbett K. D. and Brown A. V. 1975. *Geological atlas 1:250,000 series, Queenstown*. Geological Survey of Tasmania, Department of Mines.
- Corbett K. D., Pemberton J., and Vicary M. J. 1993. *Geology of the Mt. Jukes-Mt. Darwin area, 1:25,000 Map 13*. Geological Survey of Tasmania, Department of Mines.
- Crawford A. J. and Berry R. F. 1992. Tectonic implications of late Proterozoic-early Palaeozoic igneous rock associations in western Tasmania. *Tectonophysics* 214:37–56.
- Ford R. J. 1972. A possible impact crater associated with Darwin glass. *Earth and Planetary Science Letters* 16:228–230.
- Gentner W., Kirsten T., Storzer D., and Wagner G. A. 1973. K-Ar and fission track dating of Darwin crater glass. *Earth and Planetary Science Letters* 20:204–210.
- Gill E. D. and Banks M. R. 1950. Silurian and Devonian stratigraphy of the Zeehan area, Tasmania. *Papers and Proceedings of the Royal Society of Tasmania*. pp. 259–271.
- Gould C. 1866. On the position of the Gordon Limestone relative to other Palaeozoic formations. *Papers and Proceedings of the Royal Society of Tasmania*. pp. 63–66.
- Hergt J. M., McDougall I., Banks M. R., and Green D. H. 1989. Igneous rocks: Jurassic dolerite. In *Geology and Mineral resources of Tasmania*, edited by Burrett C. F. and Martin E. L. Geological Society of Australia Special Publication #15. pp. 375–409.
- Howard K. T. and Haines P. W. 2007. Geology of Darwin crater, western Tasmania, Australia. *Earth and Planetary Science Letters* 260:328–339.
- Howard K. T. 2004. *Origin of Darwin glass*. Ph.D. thesis, University of Tasmania, Hobart, Australia. 362 p.
- Howard K. T. 2003. Geochemical systematics in Darwin impact glass (abstract #5079). *Meteoritics & Planetary Science* 38:A47.
- Howard K. T. and Haines P. W. 2003. Distribution and abundance of Darwin impact glass (abstract # 4057). *Proceedings of the Third International Conference on Large Meteorite Impacts*.
- Koerberl C., Reimold W. U., Blum J. D., and Chamberlain C. P. 1998. Petrology and geochemistry of target rocks from the Bosumtwi impact structure, Ghana, and comparison with Ivory Coast tektites. *Geochimica et Cosmochimica Acta* 62:2179–2196.
- Loh C. H., Howard K. T., Chung S. L., and Meffre S. 2002. Laser fusion $^{40}\text{Ar}/^{39}\text{Ar}$ ages of Darwin Impact glass. *Meteoritics & Planetary Science* 37:1555–1562.
- Meisel T., Koerberl C., and Ford R. J. 1990. Geochemistry of Darwin impact glass and target rocks. *Geochimica et Cosmochimica Acta* 54:1463–1474.
- Raheim A. and Compston W. 1977. Correlations between metamorphic events and Rb-Sr ages in metasediments and eclogite from western Tasmania. *Lithos* 10:271–289.
- Rock N. M. S. 1991. *Lamprophyres*. Glasgow, UK: Blackie. 285 p.
- Schaaf P. and Müller-Sohnius D. M. 2002. Strontium and neodymium isotopic study of Libyan Desert Glass: Inherited pan-African age signatures and new evidence for target material. *Meteoritics & Planetary Science* 37:565–576.
- Shaw H. F. and Wasserburg G. J. 1982. Age and provenance of the target materials for tektites and possible impactites as inferred from Sm-Nd and Rb-Sr systematics. *Earth and Planetary Science Letters* 60:155–177.
- Sun S.-S. and McDonough W. F. 1989. Chemical and isotopic systematics of oceanic basalts: Implications for mantle composition and processes. In *Magmatism in the ocean basins*, edited by Saunders A. D. and Norry M. J. London: Geological Society. pp. 313–345.
- Whitehead J., Papanastassiou D. A., Spray J. G., Grieve R. A. F., and Wasserburg G. J. 2000. Late Eocene impact ejecta: Geochemical and isotopic connections with the Popigai impact structure. *Earth and Planetary Science Letters* 181:473–487.
- Whitford D. J., Crawford A. J., Korsch M. J., and Craven S. J. 1990. Strontium and neodymium isotopic studies of the Mount Read volcanics, Tasmania. *Proceedings of Tenth Australian Geologic Convention*. Geologic Society of Australia. pp. 215–216.
- Williams E. A. 1989. Summary and synthesis. In *Geology and mineral resources of Tasmania*, edited by Burrett C. F. and Martin E. L. Geological Society of Australia Special Publication #15. pp. 468–515.